International Journal of Thermophysics, Vol. 26, No. 1, January 2005 (© 2005)
DOI: 10.1007/s10765-005-2375-x

Analysis of the Piezoelectric Photothermal Spectra of $Cd_{1-x}Mn_xTe$ Mixed Crystals[1]

M. Malinski,[2,3] J. Zakrzewski,[4] S. Legowski,[4] and H. Meczynska[4]

In this paper, the analysis of the piezoelectric photothermal (PPT) spectra of a series of $Cd_{1-x}Mn_xTe$ mixed crystals is presented. The results indicated that the investigated mixed crystals exhibited nonuniform composition which is the result of diversified spatial distribution of manganese ions in the samples. Computations of the piezoelectric spectra, performed in multi-layer models of real samples, enabled determination of the percentage compositions of crystals in the two crystal regions approach. Different types of spatial distribution of manganese in the samples were revealed. Application of the models also enabled a quantitative estimation of the state of the surface of investigated samples.

KEY WORDS: mixed crystals; piezoelectric detection; semiconductors.

1. INTRODUCTION

Mixed AII–BVI crystals are promising materials for optoelectronics as it is possible to tune their crystal and optical parameters by changes of composition. Adding Be, Mn or Mg to AII–BVI materials causes almost linear changes of the value of their energy gap [1–3]. For analysis of properties of these crystals, photoacoustic techniques were applied. Microphone and piezoelectric photothermal (PPT) detection turned out to be useful for the analysis of both thermal and optical parameters [4, 5], especially

[1]Paper presented at the Fifteenth Symposium on Thermophysical Properties, June 22–27, 2003, Boulder, Colorado, U.S.A.

[2]Department of Electronics, Technical University of Koszalin, 17 Partzantow Street, 75-411 Koszalin, Poland.
[3]To whom correspondence should be addressed. E-mail: mmalin@tu.koszalin.pl
[4]Instytut Fizyki, Uniwersytet Mikolaja Kopernika, ul. Grudziadzka 5/7, 87–100 Torun, Poland.

for mixed crystals. In recent years evolving from a qualitative method, these methods have now become quantitative, and when both the amplitude and phase spectra are considered, a precise analysis of the structure of the spectra becomes possible [6,7]. Computations of the spectra not only enabled extraction of a series of basic thermal and optical parameters of samples, but also revealed the complex physical structure of samples, i.e., their inhomogeneous composition and destruction of their surfaces being the result of different after-growth thermal, mechanical, and chemical treatment.

$Cd_{1-x}Mn_xTe$ mixed crystals are a class of AII–BVI semi-magnetic semiconductors that contain transition metal Mn ions in the Cd cation sites. This group of materials is promising since by varying the Mn concentration, it is possible to tune the fundamental band gap value in the range from 1.5 to 2.5 eV [5,8]. The objective of this study is to determine what other changes are caused by Mn admixture apart from the shift of the energy gap value. One of the issues of interest was the uniformity of the composition of crystals grown with the admixture of Mn ions and the compositional broadening of the optical absorption band for the energy of photons below the energy gap value in the so-called Urbach edge region. All numerical computations of the PPT spectra presented in this paper were performed with modified Jackson–Amer [9] and Blonskij et al. [10] models with a different temperature spatial distribution formula [11,12]. Results of preliminary computations of the PPT spectra indicated, however, that it was not possible to reproduce experimental PPT spectra in a single-layer model of samples. Finally the spectra were computed in different multi-layer models of real samples [13,14], and this approach turned out to be successful indicating the complex physical structure of investigated samples. For computations, fitting procedures were applied to determine some optical parameters. These parameters are necessary for a description of optical absorption coefficient spectra. The formulae applied for computations were given by the following expressions:

$$\text{for } E_{\text{exc}} < E_{\text{g}} \quad \beta(h\nu) = \beta_0 \exp[(E_{\text{exc}} - E_{\text{g}})\gamma/(kT)] \tag{1}$$

$$\text{for } E_{\text{exc}} > E_{\text{g}} \quad \beta(h\nu) = A_0\sqrt{E_{\text{exc}} - E_{\text{g}}} + \beta_0. \tag{2}$$

The symbols have the following meanings: E_{g} is the energy gap, E_{exc} is the excitation energy, γ is the thermal broadening coefficient of the absorption band, k is the Boltzmann constant, T is the temperature, and β_0 and A_0 are proportionality coefficients. The thermal parameters of the investigated samples that were necessary for computations of the PPT spectra were determined by the phase method [15].

2. EXPERIMENT

$Cd_{1-x}Mn_xTe$ mixed crystals were grown by the high-pressure Bridgman method [16]. The investigated crystals exhibited average Mn concentration $x = 0, 0.27, 0.49, 0.67$ (mole fractions) and a zinc blende crystallographic structure. The PPT spectra were measured in the rear excitation configuration in an open cell [17] with a lock-in amplifier (Stanford SR 510) using a wave conversion method. For the measurements of the PPT spectra, a xenon lamp (Cermax 300 W) was used. All measurements were performed at room temperature.

3. RESULTS AND DISCUSSION

The photoacoustic (PA) technique has already been applied for investigations of CdTe crystals with piezoelectric detection [18, 19] as has also been done with the microphone method for $Cd_{1-x}Mn_xTe$ [20]. It was expected that PA experiments could yield information about the quality and composition of samples.

Piezoelectric photothermal (PPT) amplitudes and phase spectra of CdTe crystals measured at room temperature for the frequency of modulation $f = 76$ Hz and the thickness of samples $l = 0.1$ cm are shown in Fig. 1.

It was possible to investigate the influence of the thicknesses of the uppermost surface layer of the sample on the piezoelectric photothermal spectra of semiconductor samples. The changes of the amplitude spectra caused by different thicknesses of the surface layer, computed for CdTe crystals, are shown in Fig. 2. This figure shows that the surface layer, called an inactive layer, modifies the high absorption region of the spectra and practically does not influence the low absorption part of the spectra. Computations of the PPT spectra of CdTe crystals presented in Figs.1 and 2 were performed with an inactive layer model. The diagram of the sample in this model is presented in Fig. 3.

The main idea of an inactive layer model is that the thermal reflection coefficient between the inactive layer and the interior of the crystal $R = -1$ where $R = (e_s - e_i)/(e_s + e_i)$ and e_s is the thermal effusivity of the surface layer and e_i is the thermal effusivity of the interior of the crystal. It is the case when the thermal effusivity of an inactive layer is lower than the thermal effusivity of the interior of the sample. Most often it is the result of the lower thermal conductivity of the surface layer caused by the mechanical treatment. As a result, thermal waves that are originally generated in the area of a thin inactive layer and resulting from multiple reflections, with $R = -1$, are almost completely damped and do not contribute to the total piezoelectric signal. This phenomenon is responsible

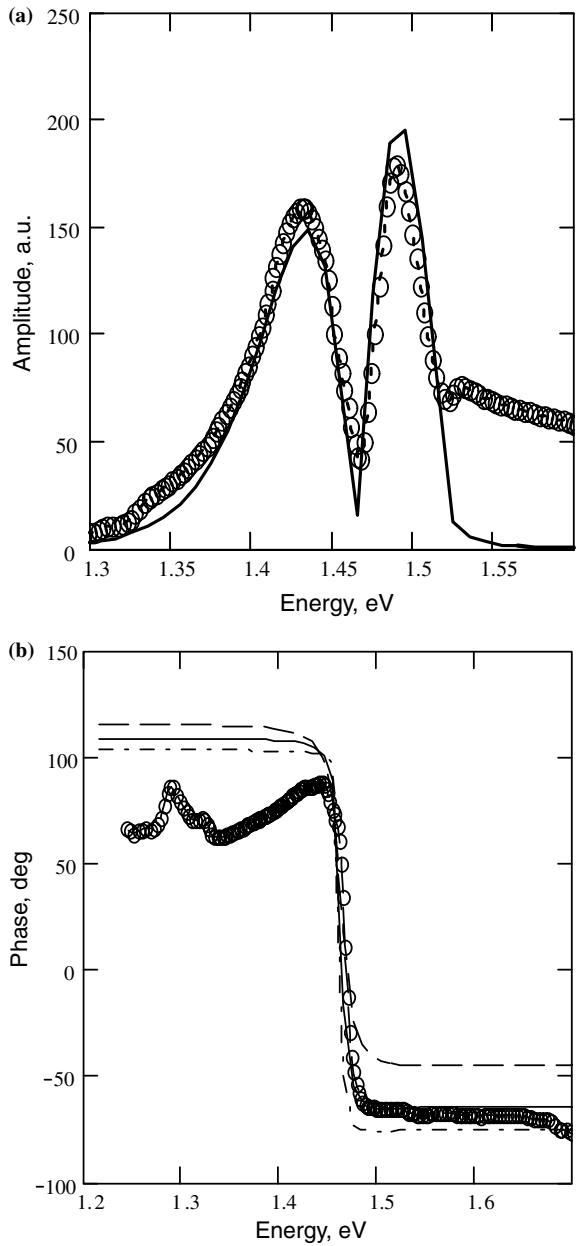

Fig. 1. (a) Amplitude PPT spectra of CdTe crystals at RT and $f = 76\,\text{Hz}$. Fitting parameters: $E_g = 1.51\,\text{eV}$, $\beta_0 = 130\,\text{cm}^{-1}, \gamma = 0.9, \alpha = 0.03\,\text{cm}^2\cdot\text{s}^{-1}$, and $\Delta = 0.019\,\text{cm}$; circles–experimental results, solid line–theoretical curve. (b) Phase PPT spectra of CdTe crystals at RT and $f = 76\,\text{Hz}$. Circles–experimental results, lines–theoretical curves computed for: dashed line–$\alpha = 0.2\,\text{cm}^2\cdot\text{s}^{-1}$, solid line–$\alpha = 0.10\,\text{cm}^2\cdot\text{s}^{-1}$, dashed-dotted line–$\alpha = 0.05\,\text{cm}^2\cdot\text{s}^{-1}$; and $R_b = -0.6$. All other parameters are the same as for the amplitude spectra.

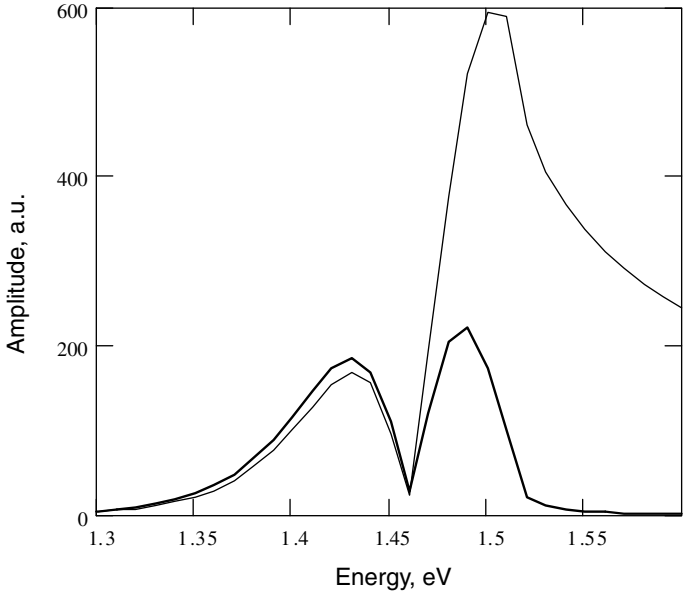

Fig. 2. Theoretical PPT amplitude spectra of CdTe crystal for two thicknesses of the inactive layer, $\Delta 1 = 0.019\,\text{cm}$ (thick solid line) and $\Delta 2 = 0.004\,\text{cm}$ (thin solid line); $f = 76\,\text{Hz}$ and $l = 0.1\,\text{cm}$.

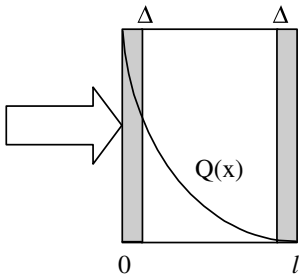

Fig. 3. Schematic diagram of a sample in an inactive-layer model. Description: l is the thickness of the sample, Δ is the thickness of an inactive layer, and $Q(x)$ is the spatial distribution of the heat sources originally generated in the sample.

for the fast decrease of the amplitude of the piezoelectric signal of CdTe samples for energies above 1.5 eV. The piezoelectric spectrum behaves as if the intensity of light-generating thermal waves in the interior of the crystal decreased according to the following formula:

$$I(h\nu) = I_0 \left(1 - \int_0^{\Delta} \exp(-\beta(h\nu)) \cdot \beta(h\nu) dx \right) \tag{3}$$

Investigated CdTe samples exhibited a value of the energy gap $E_g = 1.51$ eV close to the literature data $E_g = 1.5$ eV at RT [21]. These crystal samples exhibited, at the same time, damages of the surface determined by the thickness of an inactive layer $\Delta = 0.019$ cm. The phase spectra indicated a value of the thermal diffusivity α in the range of 0.05–0.1 $\text{cm}^2 \cdot \text{s}^{-1}$. The literature value is about 0.03 $\text{cm}^2 \cdot \text{s}^{-1}$ [22]. The PPT amplitude spectrum exhibits two peaks, one at 1.425 eV (low absorption peak) and the other at 1.5 eV (high absorption peak). The analysis of the spectra leads to the conclusion that none of the peaks is connected with any special electron levels below the energy gap of CdTe. The high-energy peak is the result of the surface damage of CdTe samples, and its position depends on the mechanical treatment of the surface. This damaged layer, called an inactive layer, is a trap for thermal waves that are originally generated in this layer, and they do not contribute to the total piezoelectric spectrum. The peak observed in the low absorption region is the result of the applied rear experimental configuration when the measured piezoelectric signal S is the difference of thermal expansion (TE) and thermoelastic bending (TEB) contributions $S = \text{TE} - \text{TEB}$. For an energy $E = 1.42$ eV, the difference, TE − TEB, reaches a maximum value. The minimum at about 1.47 eV, called a dip, is caused by compensation of the TE effect contribution by the TEB effect. As a result, two regions are observed. For energies below 1.47 eV, the thermal expansion contribution dominates, while above 1.47 eV, the thermoelastic bending contribution dominates in the piezoelectric spectrum.

PPT spectra of $Cd_{0.73}Mn_{0.27}Te$ mixed crystals are presented in Fig. 4. Computations for this case were performed with a single-layer model presented in Fig. 5. In this model, it is assumed that the whole volume of the sample exhibits the same thermal and optical parameters. In this case, single-layer model approaches of Jackson and Amer [9] and Blonskij et al. [10] can be applied. The piezoelectric spectra computed in the single-layer model are shown in Fig. 4 by a solid line. Adding manganese at a concentration $x = 0.27$ to CdTe crystals caused a shift of the energy gap E_g from 1.51 to 1.91 eV. Mixed $Cd_{0.73}Mn_{0.27}Te$ crystals exhibit smaller

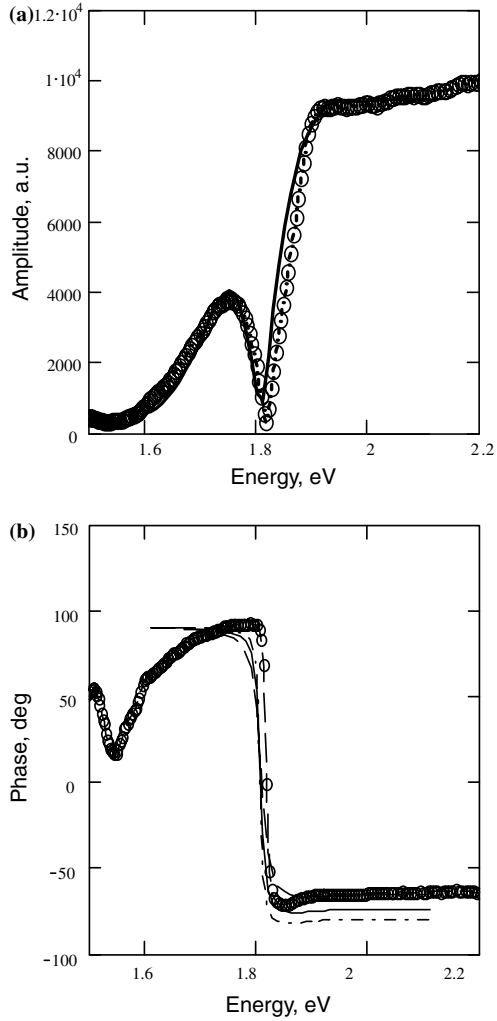

Fig. 4. (a) Amplitude PPT spectra of $Cd_{0.73}Mn_{0.27}Te$ mixed crystals measured at $f = 76\,\text{Hz}$; the thickness of samples was $l = 0.15\,\text{cm}$. Fitting parameters: $Eg = 1.91\,\text{eV}$, $\beta_0 = 150\,\text{cm}^{-1}$, $\gamma = 0.5$, $\alpha = 0.1\,\text{cm}^2\cdot\text{s}^{-1}$, $R = 1$, and $\Delta = 0\,\text{cm}$; circles–experimental results, solid line–theoretical curve. (b) Phase PPT spectra of the same sample. The same fitting parameters were applied for the computations of theoretical curves. Circles–experimental results; description of theoretical curves: dashed line–$\alpha = 0.2\,\text{cm}^2\cdot\text{s}^{-1}$, solid line–$\alpha = 0.10\,\text{cm}^2\cdot\text{s}^{-1}$, dashed–dotted line–$\alpha = 0.05\,\text{cm}^2\cdot\text{s}^{-1}$; and $R = 1$.

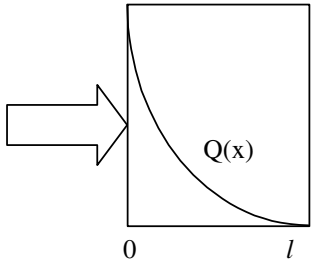

Fig. 5. Schematic diagram of a single-layer model of a sample.

thicknesses of an inactive layer equal in practice to $\Delta = 0\,\text{cm}$. Phase spectra also show an increase of the thermal diffusivity of samples. A further increase of manganese concentration in the investigated crystals generated different types of inhomogeneities in its spatial distribution as described below. Amplitude and phase PPT spectra of the mixed $Cd_{0.51}Mn_{0.49}Te$ crystals measured at RT and at $f = 76\,\text{Hz}$ are presented in Fig. 6. PPT spectra of these samples showed two kinds of crystal regions exhibiting energy gaps, $E_{g1} = 2.035\,\text{eV}$ and $E_{g2} = 2.105\,\text{eV}$ and different thicknesses of an inactive layer $\Delta = 0.005\,\text{cm}$ and $\Delta = 0\,\text{cm}$. Results of the analysis of the amplitude and phase PPT spectra of the above mentioned crystals are presented in Fig. 6a–f.

Computations of the spectra were performed with a model of a superposition of two PPT signals as presented in Fig. 7. In this model, it is assumed that the PPT signal is a superposition of two piezoelectric signals coming from two independent crystal regions I and II with the weighing factor k describing the volume contribution of each of the crystal regions;

$$S(h\nu) = S_1(h\nu)k + S_2(h\nu)(1-k), \tag{4}$$

$S_1(h\nu)$ is the spectrum of the piezoelectric signal coming from the first crystal region, and $S_2(h\nu)$ is the piezoelectric signal spectrum coming from the second crystal region.

Each crystal region is characterized by its own set of optical parameters among which the energy gap values E_{g1} and E_{g2} are the most important. The superposition model differs from the heterogeneous sample model in that each of the crystal regions is characterized by its own thickness of inactive layer Δ_1 and Δ_2. Theoretical PPT spectra of the two crystal regions and the resulting spectrum of the sample are presented in Fig. 6.

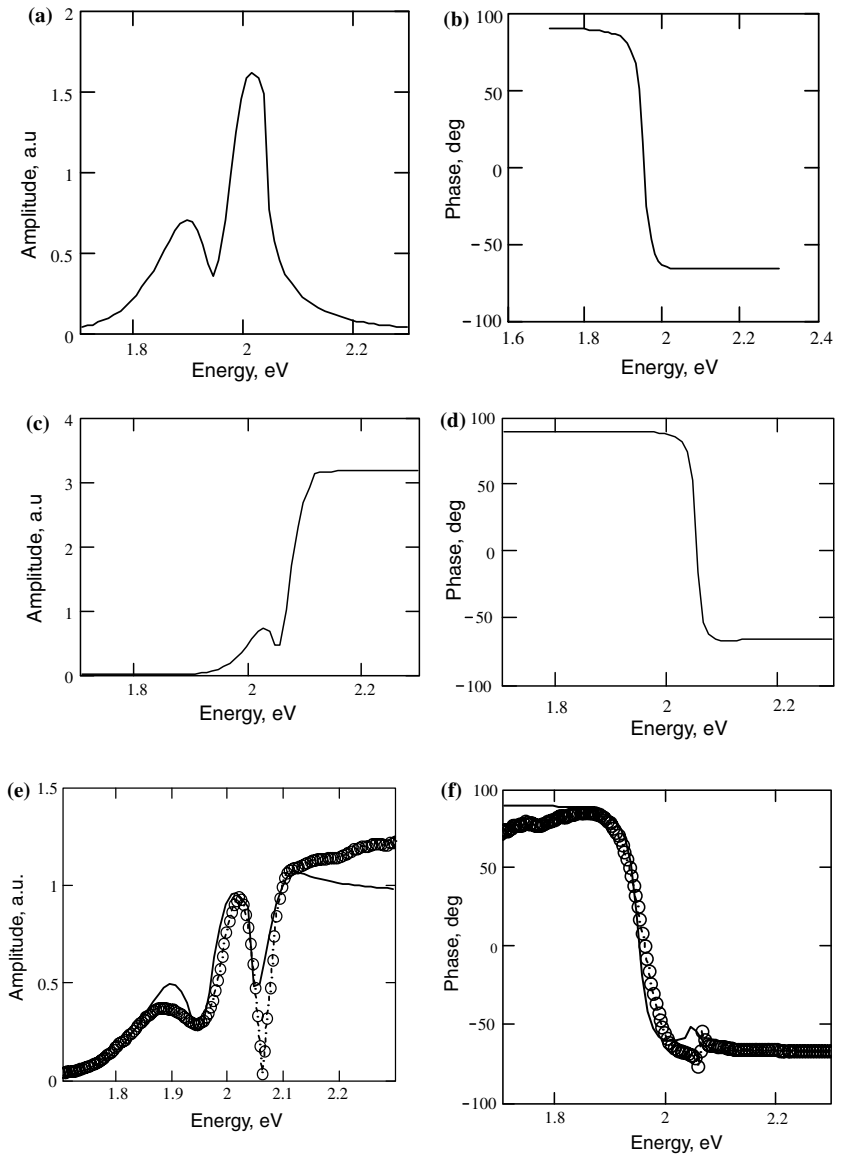

Fig. 6. (a) Theoretical amplitude and (b) phase spectra of the first crystal region: $E_{g1} = 2.035\,\text{eV}$ and $\Delta = 0.005\,\text{cm}$. (c) Theoretical amplitude and (d) phase spectra of the crystal region: $E_{g2} = 2.105\,\text{eV}$ and $\Delta = 0\,\text{cm}$. (e) Resulting theoretical amplitude and (f) phase spectra of $Cd_{0.51}Mn_{0.49}Te$ mixed crystal computed with a model of superposition for $k = 0.3$. Circles–experimental results and solid lines–theoretical curves. Fitting parameters: $E_{g1} = 2.035\,\text{eV}$, $\beta_{01} = 130\,\text{cm}^{-1}$, $\gamma_1 = 0.5$, $A_{01} = 1500$, $E_{g2} = 2.105\,\text{eV}$, $\beta_{02} = 150\,\text{cm}^{-1}$, $\gamma_2 = 0.9$, $A_{02} = 1500$, $\alpha = 0.1\,\text{cm}^2\cdot\text{s}^{-1}$, $f = 76\,\text{Hz}$, $\Delta_1 = 0.005\,\text{cm}$, $\Delta_2 = 0\,\text{cm}$, $R = 1$, and $k = 0.3$.

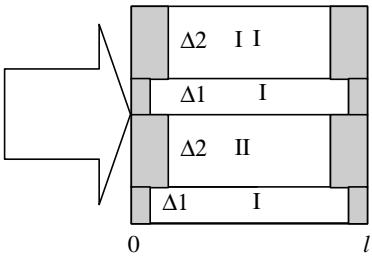

Fig. 7. Schematic diagram of the sample in a model of superposition of two PPT signals.

A further increase of the manganese concentration caused another qualitative change of the character of the spatial distribution of manganese in the samples. The experimental and theoretical PPT spectra of $Cd_{0.33}Mn_{0.67}Te$ mixed crystals are presented in Fig. 8a–f.

Amplitude of PPT spectra show the presence of two different crystal regions exhibiting energy gaps, $E_{g1} = 2.16\,eV$ and $E_{g2} = 2.34\,eV$. Computations of the spectra were performed with a model of an enriched layer. In this model, crystal regions exhibiting different values of energy gaps are placed in a layer configuration as shown in Fig. 9. In this model it is assumed that the concentration of manganese in the upper layer of a sample of thickness of about $\Delta_2 = 0.020\,cm$ is greater than in the interior of the sample which results in a larger value of its energy gap equal to $E_{g2} = 2.34\,eV$. The interior of the crystal is characterized by the energy gap $E_{g1} = 2.16\,eV$ and the thickness $\Delta_1 = 0.0017\,cm$. It is responsible for the decrease of the amplitude of the PPT signal for photon energies above 2.3 eV (see Fig. 8e).

The spectral analysis presented above enabled an estimation of the composition of samples. This analysis was possible as a result of the calibration characteristic shown in Fig. 10, where the dependence of the energy gap value of the $Cd_{1-x}Mn_xTe$ mixed crystals on the concentration of manganese is presented. Application of multi-layer models in the numerical analysis of the amplitude and phase PPT spectra enabled determination of the composition of the samples. Results of computations are presented in Table I.

4. CONCLUSIONS

Results of the piezoelectric spectral analysis of the mixed crystals $Cd_{1-x}Mn_xTe$ indicated that their composition exhibits nonuniform character. A need for explanation of the characteristic features of the observed

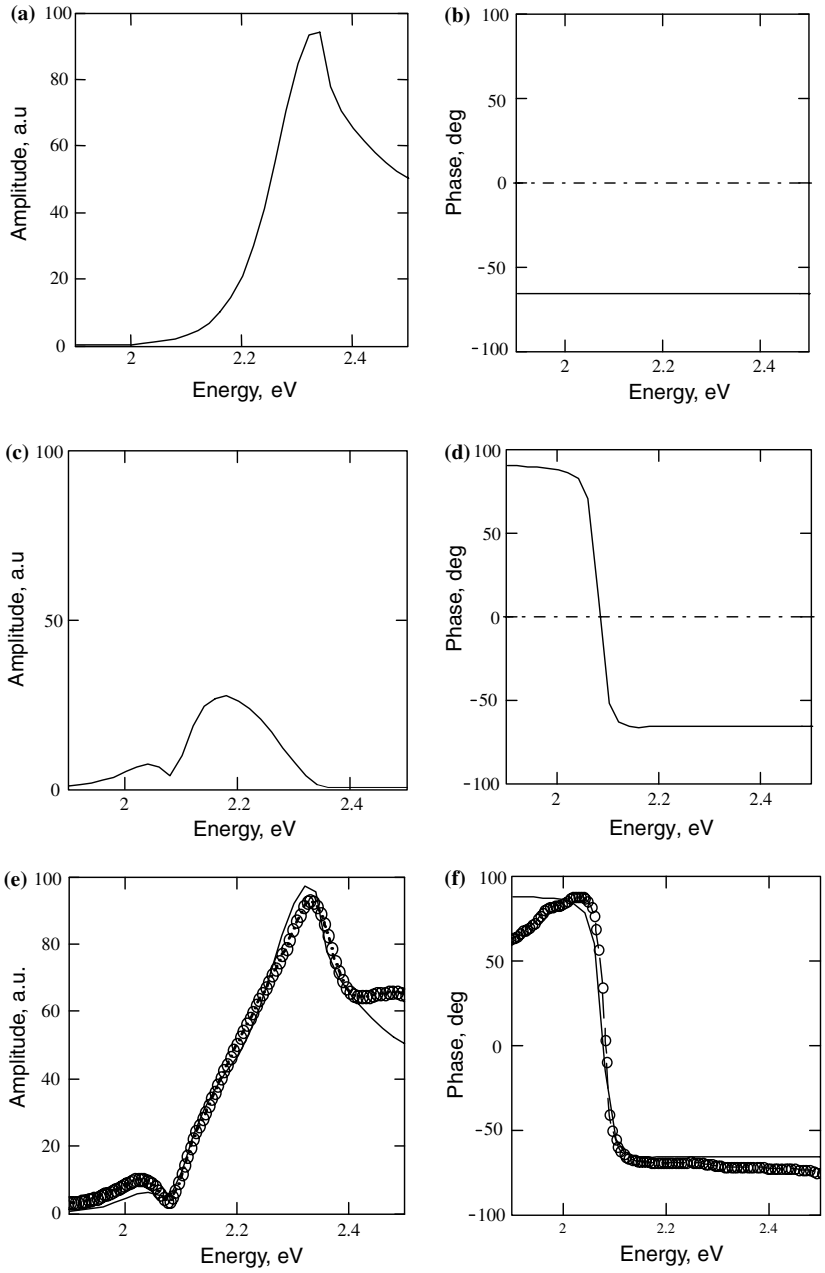
(a)
Amplitude, a.u
Energy, eV
(b)
Phase, deg
Energy, eV
(c)
Amplitude, a.u
Energy, eV
(d)
Phase, deg
Energy, eV
(e)
Amplitude, a.u.
Energy, eV
(f)
Phase, deg
Energy, eV

◀ **Fig. 8.** Amplitude and phase PPT spectra of $Cd_{1-x}Mn_xTe$ mixed crystals for $x = 0.67$, $l = 0.1$, and $f = 76$ Hz. Fitting parameters: $E_{g1} = 2.16$ eV, $E_{g2} = 2.34$ eV, $\gamma_1 = 0.5$, $\gamma_2 = 0.5$, $\beta_{01} = 150\,cm^{-1}$, $\beta_{02} = 150\ cm^{-1}$, $\Delta_1 = 0.0017$ cm, $\Delta_2 = 0.020$ cm, $\alpha = 0.1$, and $R = 1$. Circles–experimental results, solid lines–theoretical curves. Theoretical (a) amplitude and (b) phase spectra of the PPT signal contribution resulting from the light absorption in the enriched layer of thickness, $\Delta_2 = 0.020$ cm (region II); theoretical (c) amplitude and (d) phase spectra of the PPT signal coming from the light absorption in the interior of the crystal (region I); experimental and theoretical (e) amplitude and (f) phase spectra of the crystal from the result of superposition of the two contributions.

PPT spectra brought about the application of a few multi-layer models. For a numerical description of the PPT spectra, the following models were applied: a single-layer model for $x = 0.27$, an inactive-layer model for $x = 0$, a model of superposition for $x = 0.49$, and an enriched-layer model for $x = 0.67$. These models demonstrate the complexity of the physical structure of analyzed samples. Application of these models enabled the deter-

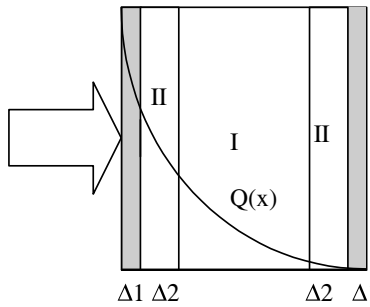

Fig. 9. Schematic diagram of a sample in a model of the enriched layer. Description: Δ_1 is the thickness of the inactive layer, and Δ_2 is the thickness of the enriched layer. Assumption: $E_{g1} < E_{g2}$.

Table I. Compositions of the Samples (mol%)

Parameter x	I crystal region	II crystal region
0	CdTe 100 %	–
0.27	$Cd_{0.67}Mn_{0.33}Te$ 100%	–
0.49	$Cd_{0.58}Mn_{0.42}Te$ 70%	$Cd_{0.53}Mn_{0.47}Te$ 30%
0.67	$Cd_{0.47}Mn_{0.53}Te$ 60%	$Cd_{0.34}Mn_{0.66}Te$ 40%

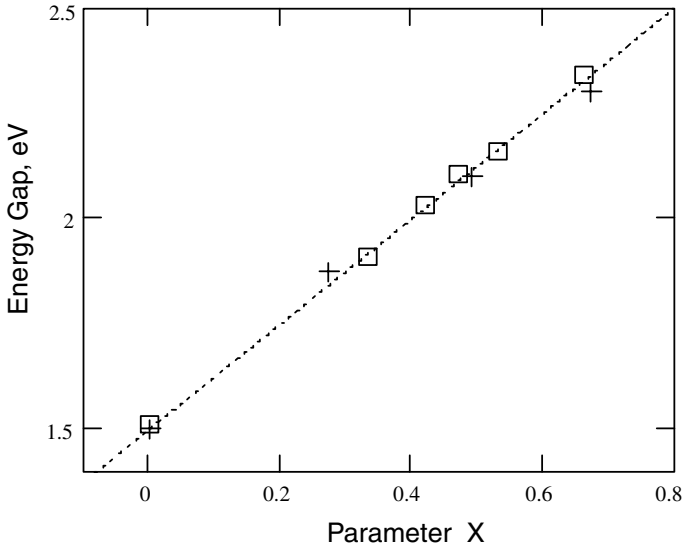

Fig. 10. Dependence of the energy gap value E_g on the x parameter describing manganese concentration in the $Cd_{1-x}Mn_xTe$ crystal sample. Crosses denote values of the x parameter presented in Ref. 5. Squares denote values of energy gaps extracted from the analysis of the PPT spectra of investigated samples.

mination of the compositions of crystals and a set of their basic optical parameters. The computations of the phase spectra enabled determination of the thermal diffusivities of samples without the need for separate frequency domain experiments.

REFERENCES

1. G. Landwehr, *Proc. 2nd Int. Symp. on Blue Lasers and Light Emitting Diodes*, Chiba, Japan (1998), p. 3.
2. A. Kudelski, A. Golnik, I. A. Gaj, F. V. Kyrychenko, G. Karczewski, T. Wojtowicz, Yu. G. Semenov, O. Krebs, and P. Voisin, *Phys. Rev. B* **64**:045312 (2001).
3. G. F. Goya and V. Sagredo, *Phys. Rev. B* **64**:235208 (2001).
4. Y. R. Lee, A. K. Ramdas, and R. L. Aggarwal, *Phys. Rev. B* **38**:10600 (1988).
5. J. Zakrzewski, F. Firszt, S. Legowski, H. Meczynska, A. Marasek, and M. Pawlak, *Rev. Sci. Instrum.* **74**:572 (2003).
6. M. Malinski, L. Bychto, F. Firszt, J. Szatkowski, and J. Zakrzewski, *Anal. Sci.* **17**:133 (2001).
7. M. Maliński, L. Bychto, F. Firszt, J. Szatkowski, and J. Zakrzewski, *Microelectronics J.* **32**:903 (2001).
8. J. Zakrzewski, Ph.D. thesis (UMK, Toruń, 2001).

9. W. Jackson and N. M. Amer, *Appl. Phys.* **51**:3343 (1980).
10. J. V. Blonskij, V. A. Tkhoryk, and M. L. Shendeleva, *J. Appl. Phys.* **79**:3512 (1996).
11. M. Malinski, *Arch. Acoust.* **27**:217 (2002).
12. M. Malinski, *Arch. Acoust.* **28**:43 (2003).
13. M. Malinski, *Mol. Quantum Acoust.* **23**:277 (2002).
14. M. Malinski and J. Zakrzewski, *Rev. Sci. Instrum.* **74**:598 (2003).
15. M. Malinski, *Phys. Stat. Sol. A* **198**(1):169 (2003).
16. F. Firszt, H. Meczynska, B. Sekulska, J. Szatkowski, W. Pszkowicz, and A. Kachniarz, *Semicond. Sci. Technol.* **10**:197 (1995).
17. H. D. Breuer, *Proc. 1st Int. Conf. on Photoacoustic Effect in Germany*, Vol. 115 (1981), p. 115.
18. O. Goede, W. Heimbrodt, and Th. Kopp, *Phys. Stat. Sol. A* **168**:443 (1988).
19. O. Goede, W. Heimbrodt, and F. Sittel, *Phys. Stat. Sol. A* **93**:277 (1986).
20. M. Nogaku and Y. Oka, *Jpn. J. Appl. Phys.* **30**:L1950 (1991).
21. www.semiconductors.co.uk/propiivi5410.htm
22. *Physical Data – Handbook* (Energoatomuzdat, Moscow, 1991) (in Russian).